Calibration strategy for ERS scatterometer data reprocessing

N. Manise, X. Neyt and M. Acheroy

Royal Military Academy, Brussels, Belgium

ABSTRACT

From the beginning of its mission, in 1995, the ERS-2 satellite has recorded an important set of data. The performance and accuracy of its instrument provide precious information for the scientific community. The experience acquired during 10 years has led the European Space Agency (ESA) to plan a reprocessing activity of the entire set of the available scatterometer data. This reprocessing activity will use the enhanced on-ground processing[1] and calibration[2] chains.

In this paper, the calibration strategy for the scatterometer data reprocessing from the beginning of the mission is presented. It consists in looking for a calibration area (rainforest, ocean or ice) which would allow a highly accurate tuning of the antenna patterns (already tuned within the specifications).

Keywords: Scatterometer, calibration, rainforest, reprocessing, ERS-2

1. INTRODUCTION

The scatterometers on-board ERS satellites are active real aperture radar instruments. Backscatter coefficients (σ^0) which depend on the roughness of the Earth's surface, are measured. The main application is wind-retrieval from σ^0 acquired over the oceans but some other applications like soil moisture emerged recently.

The spacecraft is yaw steered in order to limit the Doppler shift, the bandwidth of the on-board system being itself limited. Due to a malfunction of several gyroscopes in 2001, yaw steering couldn't be guaranteed anymore which leaded to a review of the scatterometer processing[1] and calibration[2] chains.

Furthermore, ERS-2 lost its on-board recording sub-system in 2003 and only measurements over Europe, North-America and West Africa are available since then. Fortunately, the coverage area has been recently increased by installing three new ground stations in Miami (Florida), Mc Murdo (Antarctica) and Beijing (China). These events have important consequences as well on the winds coverage as on the calibration monitoring.

Thanks to ten years of experience and a detailed understanding of the instrument, ESA has planned a reprocessing activity of the entire set of the available scatterometer data. The objective consists in providing to the users the most accurate products derived from the instrument, the antenna patterns being already tuned within the specifications (0.5dB). The calibration strategy for the reprocessing is exposed in this paper.

Section 2 is dedicated to the absolute calibration. Transponders at known locations (on ground) can theoretically be used to perform an absolute calibration of the instrument. Due to the gyroscopes failures, the yaw angle is unknown and the calibration algorithm has been reviewed in order to take into account the estimation of the yaw angle in the calibration chain.

Section 3 is dedicated to the relative calibration. It consists in using large stable and homogeneous areas to tune the antenna patterns of each beam, to monitor these antenna patterns in time (aging effects), and to cross-calibrate the patterns between beams. The Amazonian rainforest shows high stability over time and it has been demonstrated that it is, hence, a primary choice for relative calibration.[3] Due to the on-board recording failure, the monitoring of the antennas patterns over the rainforest is no longer possible. New calibration areas have to be found in order to insure the quality of the products. In this section, the study of the ice sheets and the ocean as calibration targets will also be developed.

Section 4 presents the strategy to re-calibrate and monitor the antenna patterns for the reprocessing and the remaining life of ERS-2.

Section 5 summarizes and concludes this paper.

Further author information: (Send correspondence to Nicolas Manise) E-Mail: Nicolas.Manise@rma.ac.be, Telephone: +32 2 737 6474, Address: Signal and Image Center, Electrical Engineering Dept., Royal Military Academy, 30 av de la Renaissance, B-1000 Brussels, Belgium

2. ABSOLUTE CALIBRATION

2.1. Introduction

Transponders are commonly used to calibrate satellites instruments. The transponders used for ERS-2 scatterometers calibration are arranged in line in the south of Spain. This position allows measurements at more than two incidence angles every three days. Their alignment has been designed such that they may be illuminated by each scatterometer antenna during an ascending or a descending pass. Moreover, several transponders might be illuminated by each beam during the same pass.[4]

Every time the satellite overflies the transponders, the wind scatterometer is configured in calibration mode, and RF pulses are transmitted to the transponders by the Fore, Mid and Aft antennas (F-M-A) during periods of 120, 40 and 120 seconds respectively.[5]

The transponders have a varying (with transponder electronics temperature) Radar Cross Section (RCS) which is measured on-ground. According to the RCS, the received RF pulses are amplified and recorded. Pulses are then re-transmitted to the spacecraft with a frequency shift of 540 kHz that permits to easily filter out clutter echo signal components. The transponders thus appear as punctual spots in the echo.[6]

The comparison between the emitted and received signals by resolving the radar equation theoretically allows an accurate calibration of the instrument.

2.2. Transponders

The relation between the emitted and received signal is governed by the radar equation:

$$P_r = KP_i\frac{G_\theta(\theta)^2 G_\phi(\phi)^2}{R^4}\sigma ERF \tag{1}$$

where P_r is the power received by the satellite, K is the gain constant with ideal value 1 (0 dB), P_i is the power emitted by the satellite, $G_\theta(\theta)$ is the gain in elevation, $G_\phi(\phi)$ is the gain in azimuth, R is the distance between the satellite and the transponder, σ is the RCS of the transponder and ERF is the external rescale factor. As σ (characteristic of the transponder) and ERF are constants, K is obtained by integration on a subregion around the echo peak.
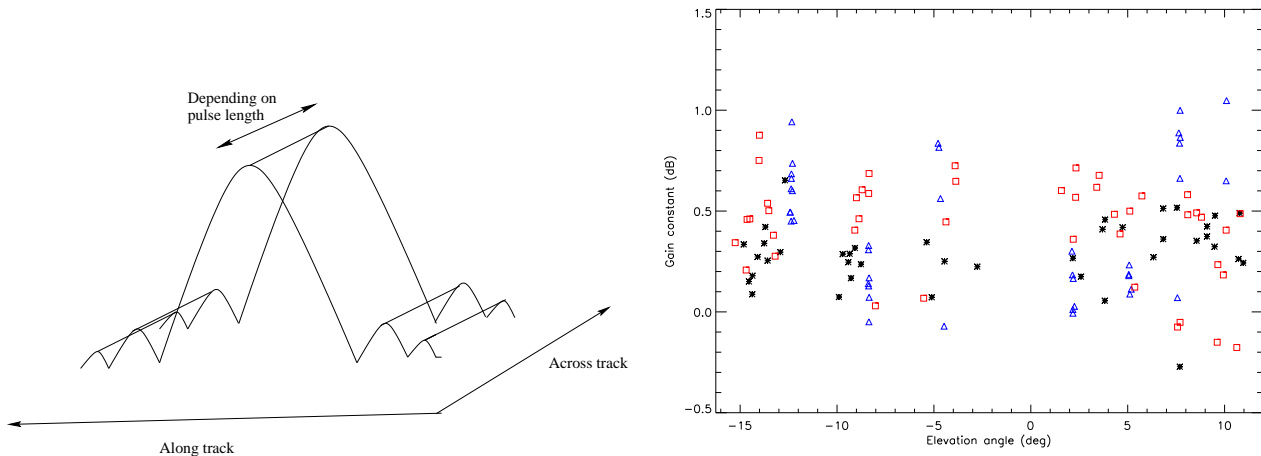

Figure 1. Left: Theoretical "on-ground" pulse shape. Along-track, the shape is governed by the azimuth antenna pattern of the antenna. Across-track, the shape is governed by the pulse length. Right: Gain constant over the incidence angle from 2001. The black stars, blue triangles and red squares respectively stand for the Fore, Mid and Aft beams.

The absolute calibration consists in determining the gain constant K which relates the signal emitted and received by the satellite. The gain constant is independent from the incidence angle: a calibrated instrument

would ideally lead to a flat and unit gain constant over the incidence angle. As the previous calibration chain was not able to deal with the large mis-pointing errors due to gyroscopes failures, a new chain had to be redeveloped.[2]

Figure 1 (right) shows the gain constant computed from 2001. Results show a high variance which is explained by two factors. First, there is not enough averaging (not enough passes over the transponders) to significantly reduce the variability of the measurements. Secondly and mostly, the on-board fast time sampling is not important enough to precisely cover the pulse's shape (see Figure 1 left). This is particularly true for the Mid-beam which has a shorter pulse length.

The calibration can therefore be monitored around 0.7dB standard deviation (std). The measurements over the transponders thus present a high variability and are not accurate enough to calibrate the scatterometers within the specifications.

3. RELATIVE CALIBRATION

3.1. Introduction

Theoretically, the transponders give measurements of antenna attenuation only at particular points within the antenna pattern. The fine tuning across all incidence angles is therefore not possible using transponders as there are simply not enough samples. This issue can be solved by using large stable natural targets.
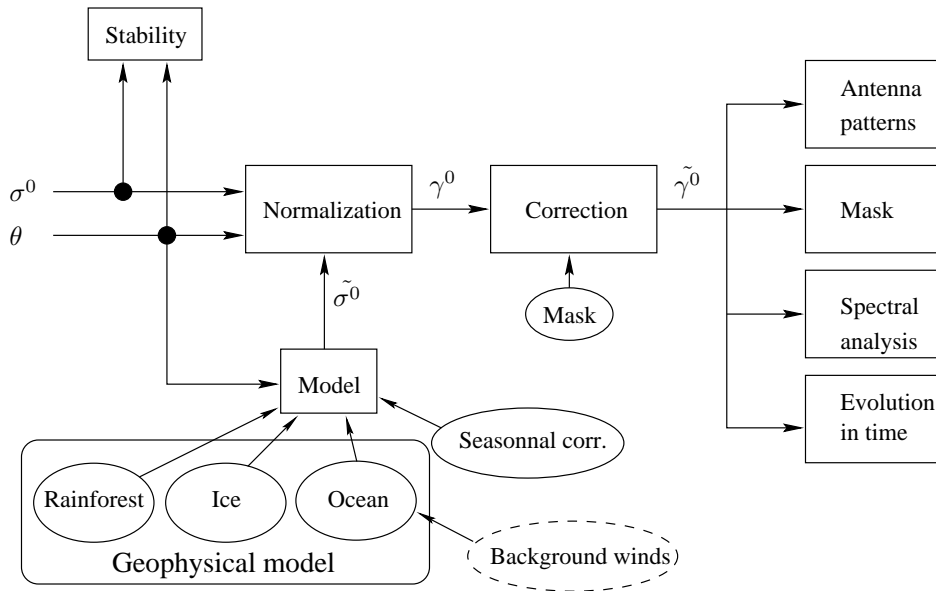

Figure 2. Diagram showing the analysis made for the relative calibration.

Figure 2 synthetizes the analysis made in this paper regarding the relative calibration.

An important feature of a calibration site is the temporal stability of the area for the measurements to be comparable in time. This can be done by measuring the variance of the σ^0 for the different incidence angles (θ) at the same location. For instance, the Amazonian rainforest shows high stability over time and it has already been proved that it is suitable for relative calibration.[3] Due to the on-board recording sub-system failure in 2003, data over the rainforest is not available anymore. Hence, other calibration sites such as Greenland or Antarctica which are in investigation for calibration[7] are also studied in this paper.

Once a stable area has been found, the normalization consists in applying a model ($\tilde{\sigma^0}$) to the σ^0. This provides a backscatter coefficient called γ^0. The model which is applied depends on the calibration area. For the rainforest, the constant gamma model is usually applied to perform the normalization. This model theoretically removes the effect of the incidence angle on the σ^0 but assumes an isotropic and homogeneous target.[4] Empirical

models could be used on the ice sheets. It was shown that the calibration of the antenna patterns might also be performed over the ocean.[8] The normalization is then performed using reference $\tilde{\sigma}^0$ which are derived from reference winds using a wind model.[9] A seasonal correction which compensates for seasonal effects could also be integrated in the model.

From the γ^0, a spatial mask could remove the undesirable targets. This technique is in particular used over the rainforest to make the rainforest as homogeneous as possible.

$\tilde{\gamma}^0$ is thus a normalized σ^0 where all corrections concerning the calibration area or mission scenarios (hence not related to the antenna patterns themselves) are applied. From $\tilde{\gamma}^0$, antenna patterns and a spatial mask will be derived. A spectral and a temporal analysis will also be performed.

3.2. Stability

Figure 3 shows the stability of σ^0 over the rainforest (top) Greenland (middle) and Antarctica (bottom). Areas have been gridded and the variance computed for each beam over a period of 18 months from May 1997. At first sight, the rainforest is very stable, Greenland presents a large stable area which might be useful for relative calibration[7, 10] while Antarctica has only a few stable places.
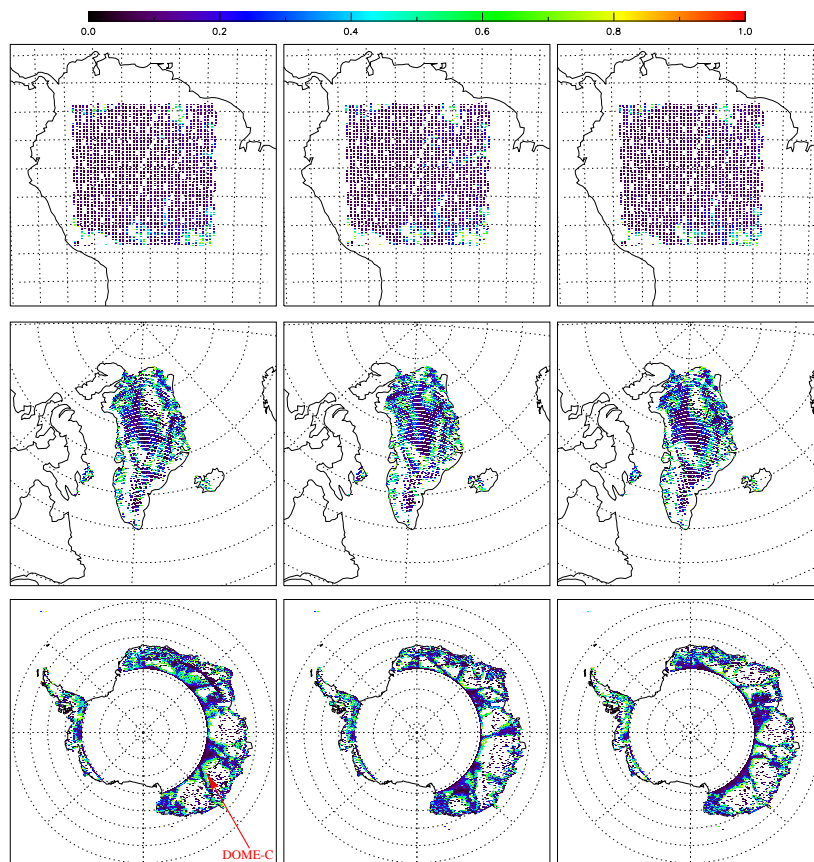

Figure 3. The areas have been gridded and the variance has been computed in each cell over 18 months from May 1997. The three pictures of each area represent the variance of σ^0 in each cell for the Fore, Mid and Aft beams. The cells with a variance higher than 1dB have not been drawn (in white). Top: The rainforest (node 1) is very stable. Middle: Greenland (node 1) shows a large stable area in the central part of the land which might be suitable for a calibration site. An accuracy of 0.5dB std (0.3dB variance) might be possible. Bottom: Antarctica (node 19) shows very few candidates for calibration.

Dome-C (Antarctica: 75S, 123E), which is currently under investigation for SAR calibration,[7] seems not to be suitable for all the beams of the scatterometer. Moreover, considering the resolution of the scatterometer, only large areas (like the rainforest) might be usable for calibration. Figure 3 (bottom) clearly shows that there are no such large areas that are stable for the three beams at the same time in Antarctica. Antarctica is therefore not a suitable calibration site for the scatterometer.

3.3. Models, normalization and corrections

3.3.1. Rainforest

Inhomogeneousness

It was shown that the rainforest is not totally homogeneous.[11] Rivers and towns respectively have a lower and a higher backscatter than the canopy. Moreover, the canopy itself is composed of various types of trees and vegetation which have different characteristics. The way to handle the inhomogeneousness of the rainforest, as shown in Figure 4 (left) is to build a mask which selects the targets of interests.

The mask is composed of all the areas inside the rainforest presenting a variance of γ^0 lower than 0.25dB and a mean value close to the mean value of the entire rainforest. Targets having a different backscatter than the canopy have successfully been removed: rivers (Rio Negro and Amazon), large towns and hilly zones inside the rainforest.
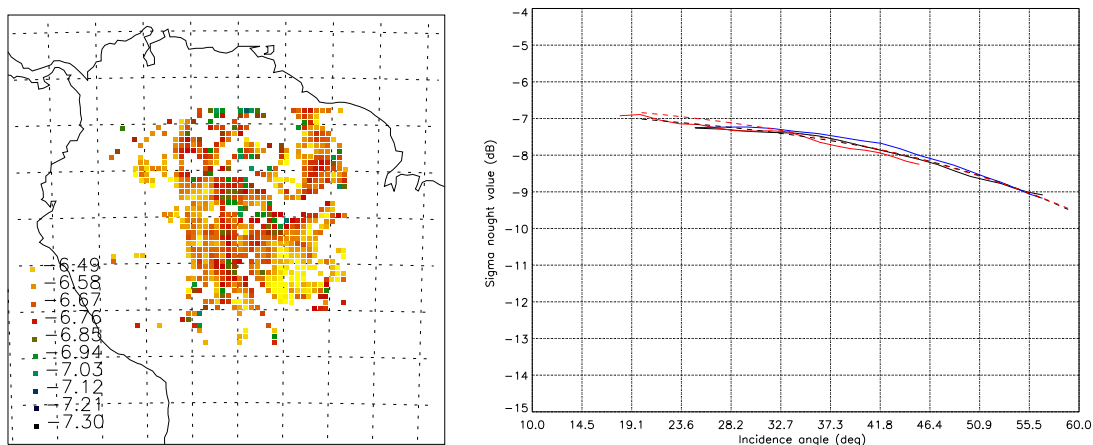

Figure 4. Left: Image (γ^0) of the rainforest with undesirable targets removed thanks to a mask. Rivers typically provide a lower backscatter while towns provide a higher backscatter than the canopy. Right: σ^0 wrt the incidence angle. The black, red and blue colors respectively stands for Fore, Mid and Aft beams. Solid lines are σ^0 measurements. The cosine law (red dashed) and a polynomial fit - third degree - (black dashed) have been overplotted.

Model

For C-Band microwaves, tropical rainforests may be regarded as pure volume scatterers for which the incoming signal is equally scattered in all directions. Consequently, the σ^0 only depends on the surface (S') effectively seen by the instrument which, in turns, depends directly on the incidence angle.

Assuming that the rainforest is homogeneous and isotropic, S' is directly linked to the incidence angle by the relation $S' = S \cos \theta$. One can define the following formula:

$$\gamma^0 = \frac{\sigma^0}{\cos \theta} \tag{2}$$

Using this relation, the γ^0 backscattering coefficients over the rainforest are independent of the incidence angle. The γ^0 over such a target should hence be flat across the entire swath, and equal in all beams.

Figure 4 (right) shows the mean σ^0 measurements wrt the incidence angle (solid lines). The cosine law (red dashed) fits the data very well. A polynomial fit (black dashed) of the third degree has also been overplotted. This model also fits well the data.

Considering its geophysical meaning, the cosine law seems therefore to be appropriate for normalization. In this paper, the rainforest model will hence make reference to the constant gamma model.

Spectral analysis

A spectral analysis was performed on a data set of about three years (from 1998 to 2000). The satellite was then working in nominal mode, meaning that we can assume that no large deviation from the nominal attitude of the satellite occurred during this period. Only small biases have been corrected for, according to the reported mission events.[12] It is assumed that the effect of the incidence angle has been totally removed by using the rainforest model. Histograms have successively been computed for periods of one week, all nodes contributing in the same manner. Peaks of histograms have been used as the reference value for the γ^0.

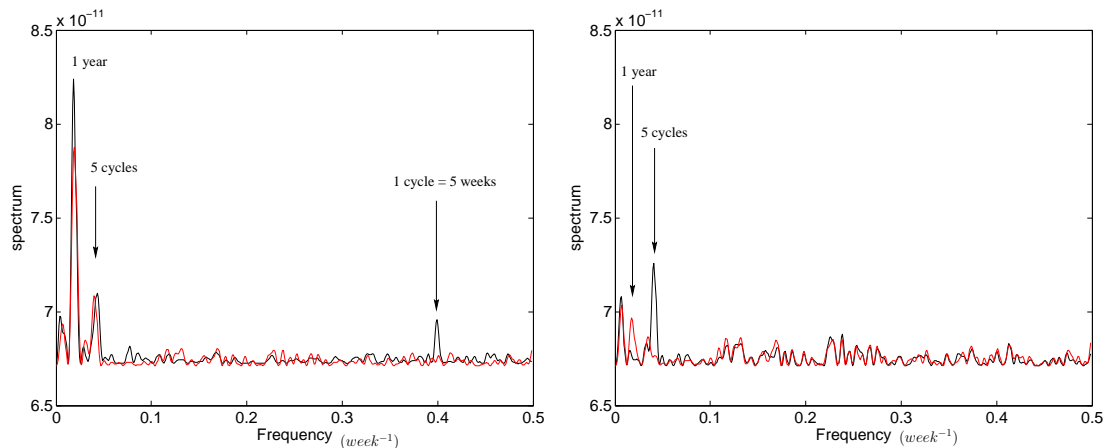The method used for the spectral analysis is the Minimum Variance Estimator (MVE).[13]

Figure 5. Spectrum of the γ^0 from 1998 to 2000, ascending passes and all nodes considered indistinctly. Left: This Figure shows the positive effect of the mask. Sub-cycle components have been removed from the spectrum (1 cycle). Right: ''Cleaned'' spectrum from the 5 cycle and 1 year components. An annual correction has been applied on the data to take into account the seasonality. The 5 cycles component is related to mission scenario and is hence independent from the antenna patterns evolution.

Figure 5 shows the results of the spectral analysis for ascending passes where all the nodes have been considered indistinctly. When no mask is applied on the data, the spectrum (left in black) clearly shows three emerging components: 1 cycle, 5 cycles and 1 year components.

The satellite overflies exactly the same area every cycle. An area having special characteristics will be lightened every cycle which will be reported in the spectrum. As shown in Figure 5 (left), the spatial mask has removed the 1 cycle component from the spectrum which is explained by the periodicity of acquisitions.

The one year component is due to the seasonal variation of the rainforest and is removed from the spectrum as shown in Figure 5 (right).

The monitoring of the SAR antenna pattern is performed every 5 cycles.[12] This modulation effect being related to the mission scenario, the 5 cycles component is removed from the spectrum.

Figure 6 shows the results of the node dependent spectral analysis for descending passes. The spatial mask has been applied and only the annual component remains (left). It is interesting to notice that the amplitude is node dependent. This underlines the imperfection of the constant gamma model. If the incidence angle effect
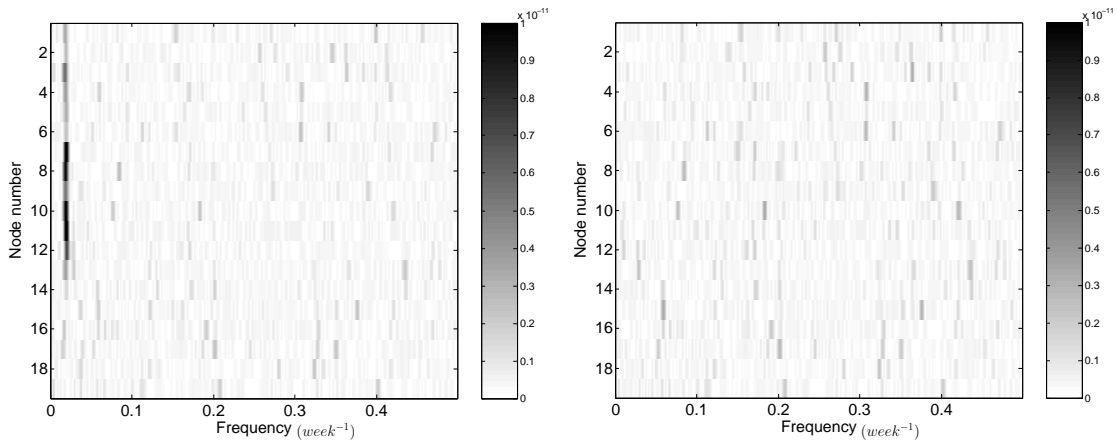
Figure 6. Spectrum of the γ^0 from 1998 to 2000, descending passes and all nodes separated. Left: No correction has been applied. The annual component is visible but has a different amplitude for each node. Right: Corrected spectrum. The node-by-node correction has been applied and the 1 year component is totally removed.

was totally removed from the data, the annual variation of the rainforest canopy would be identical for each node. The node-by-node correction of the annual variation is shown in Figure 6 (right).

These three components must be removed from the spectrum as they are inherent to the rainforest or to mission scenarios and do not correspond to any variation of the antenna patterns.

Ascending/Descending passes

When considering independently ascending and descending passes, γ^0 profiles show two types of differences. First, the mean γ^0 value is different which is explained by the difference in acquisition times, the canopy reflecting differently during day or night. Secondly, the profiles themselves are different. This might be due to local changes in backscatter in the rainforest caused by the local inhomogeneousness or by the local environmental conditions.

Figure 7 shows the influence of the corrections on the γ^0 profiles where the mean value has been removed.

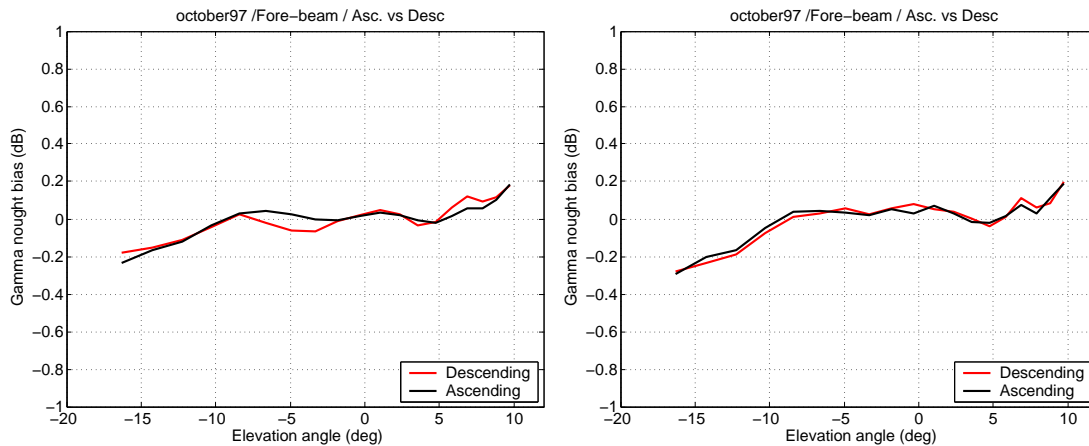**Figure 7.** γ^0 profiles in October 1997, descending passes, Fore-beam. Left: No correction was applied to the data. Right: All corrections (spectral and mask) were applied. Differences between ascending and descending passes have been reduced thanks to the corrections.

A measurement of this improvement has been obtained by averaging in time (from May 1997 to November 1998) the absolute value of the integrated γ^0 profiles. The results are presented in table 3.3.1.

Absolute error	Fore	Mid	Aft
No correction	0.1763 dB	0.1684 dB	0.1879 dB
With correction	0.1577 dB	0.1512 dB	0.1778 dB

3.3.2. Greenland

After having selected one of the most stable area in Greenland (75.7N 41.3W), an empirical model can be derived from the σ^0 (wrt the incidence angle) profile. This is shown at Figure 8 for ascending and descending passes. As ice sheets are not isotropic, the model cannot be beam-independent. Six models can therefore be derived from the σ^0 profiles (one per beam and distinctly for ascending or descending passes).
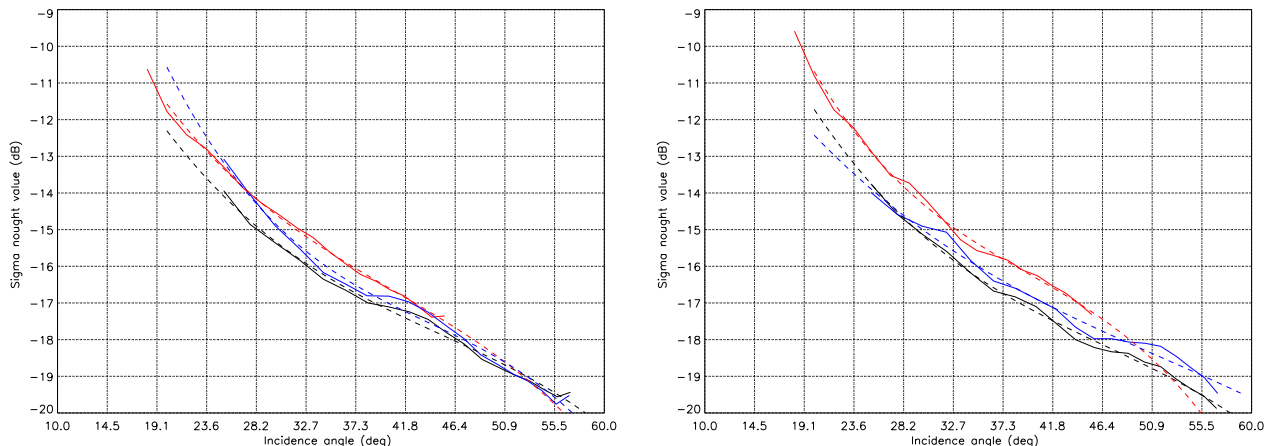

Figure 8. The black, red and blue colors respectively stands for Fore, Mid and Aft beams. The solid lines represent the σ^0 while the dashed lines are the fitted models for each beam. Left: Ascending passes. Right: Descending passes.

Models are obtained by performing a polynomial fit (third degree) on the data. These models can afterward be used to normalize the σ^0 and to derive calibrated antenna patterns. Some reserves shall here be made. First, the model cannot be derived from uncalibrated data. This calibration method could hence only be useful if the antenna patterns are tuned using another method (rainforest for instance). Nevertheless, it can be used for monitoring after fine tuning of the antenna patterns. Secondly, the central part of Greenland is subjected to very strong winds which produce erosional features on the scale of a few meters known as Sastrugi.[14] The height and alignment of the sastrugi can strongly influence the level of backscatter according to the look angle. A change in the prevailing wind direction could cause a change in the alignment of the surface features, hence in the backscatter.

The target of tuning the antenna patterns at an accuracy of less than 0.5dB standard deviation (std) is thus not achievable using ice sheets in Greenland.

3.3.3. Ocean

The ocean calibration consists in comparing the average of the measured backscatter coefficients σ^0_M to the coefficients σ^0_S obtained with collocated wind data (wind speed and direction) and the wind model that has been adopted by ESA.[9] This transfer function links a triplet (wind speed, wind direction, incidence angle) to a σ^0.

The main difficulty consists in using a collocation wind data set with uniform wind direction distribution which insures that the results are independent of errors in the harmonic terms of the transfer function, and

insensitive to uncertainty in wind direction.[8]   To remove the wind direction modulation for all wind speeds, the method consists in determining the probability distribution $p(\phi|V)$ having a wind direction ϕ for a particular wind speed V, and subsequently removing randomly a fraction of the data such that the resulting $p(\phi|V)$ becomes as uniform as possible.
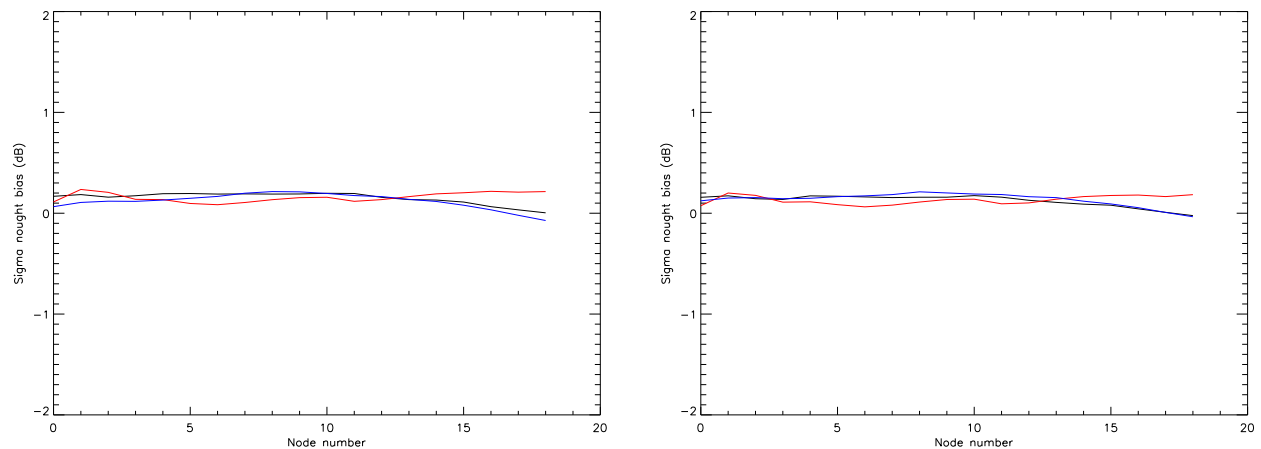

Figure 9. Ocean calibration in October 1998. The black, red and blue colors respectively represent the Fore, Mid and Aft beams. ECMWF interpolated meteorological wind speeds and directions have been used as reference data. The wind model selected is CMOD5.

The main advantage of the ocean calibration with respect to the other methods (transponders and rainforest) is the much shorter time period over which accurate results can be obtained. Only a few orbits are necessary to perform an ocean calibration. The main drawback comes from the use of an empirical wind model and of an imperfect reference wind data.

In Figure 9, the bias between σ_M^0 and σ_S^0 indicates that the σ_S^0 underestimate the measurements. One can notice the slight differences between ascending (left) and descending (right) passes. It should be noted that the antenna patterns do not have the same profile as the ones obtained with the rainforest. This might come from the imperfect rainforest model, the empirical nature of the wind model or the imperfect reference data.

The ocean calibration is expected to be accurate at 0.4dB std which could be used for the monitoring of the antenna patterns.

4. CALIBRATION STRATEGY

According to the here above analysis, the calibration strategy could be divided in two parts.

The rainforest could be used to re-calibrate accurately the antenna patterns before the on-board recording sub-system failure. It was shown that the differences between the ascending and descending passes are reduced when using the mask and removing the appropriate spectral components from the data. The ocean calibration could also be used for comparison purposes.

After the on-board recording sub-system failure, the rainforest data being not available, the ocean calibration method has shown its usefulness for monitoring purposes.

Table 4 summarizes the calibration and monitoring activities in an increasing order of priority.

5. CONCLUSIONS

Ten years after the launch of ERS-2, ESA has planned a reprocessing activity which partly consists in re-calibrating the antenna patterns. After the failure of the on-board recording sub-system, the rainforest which

Calibration technique	std	Activity
Transponders	> 0.7dB	Not usable
Ice sheets	> 0.5dB	Not usable
Ocean	≤ 0.4dB	Monitoring
Rainforest	≈ 0.25dB	Calibration and monitoring

is the first choice for calibration is nowadays out of reach. A global investigation of possible calibration sites showed that the rainforest and the ocean are the best candidates for monitoring the antenna patterns.

A calibration strategy led us to select the rainforest (before the failure) for accurate re-calibration and the ocean calibration method for monitoring.

ACKNOWLEDGMENTS

REFERENCES

1. X. Neyt, P. Pettiaux, and M. Acheroy, "Scatterometer ground processing review for gyro-less operations," in *Proceedings of SPIE: Remote Sensing of the Ocean and Sea Ice 2002*, **4880**, 2002.

2. N. Manise, X. Neyt, and M. Acheroy, "Absolute calibration of the ERS-2 scatterometer in gyro-less mode using transponders," in *Proceedings of the Pan Ocean Remote Sensing Conference*, (Concepcion, Chile), 2004.

3. R. Hawkins, E. Attema, R. Crapolicchio, and P. Lecomte, "Stability of Amazon backscatter at C-Band: Spaceborne results from ERS-1/2 and RADARSAT-1," in *CEOS SAR Workshop*, 1999.

4. P. Lecomte, "ERS wind scatterometer commissioning and in-flight calibration," in *Proceedings of a Joint ESA-Eumetsat Workshop on Emerging Scatterometer Applications – From Research to Operations*, pp. 261–270, ESTEC, (The Netherlands), Nov. 1998.

5. P. Lecomte, "The ERS scatterometer instrument and the on-ground processing of its data," in *Proceedings of a Joint ESA-Eumetsat Workshop on Emerging Scatterometer Applications – From Research to Operations*, pp. 241–260, ESTEC, (The Netherlands), Nov. 1998.

6. R. Crapolicchio and P. Lecomte, "The ERS wind scatterometer mission: routine monitoring activities and results," in *Proceedings of a Joint ESA-Eumetsat Workshop on Emerging Scatterometer Applications – From Research to Operations*, pp. 285–298, ESTEC, (The Netherlands), Nov. 1998.

7. C. H. Buck, "Alternative large-scale distributed targets for SAR elevation beam pattern characterization," tech. rep., ENVISAT project, ESA-ESTEC, 2001.

8. A. Stoffelen, "A simple method for calibration of a scatterometer over the ocean," in *J. Atmos. Ocean. technol., American meteorological Society*, 1998.

9. H. Hersbach, "CMOD5 - an improved geophysical model function for ERS C-Band scatterometry," Tech. Rep. 395, ECMWF, Jan. 2003.

10. V. Wismann and K. Boehnke, "Monitoring snow properties on Greenland with ERS scatterometer and SAR," in *European Space Agency Special Publication*, **ESA SP-414**, pp. 857–861, 1997.

11. N. Manise, X. Neyt, and M. Acheroy, "Calibration of the ERS-2 scatterometer in gyro-less mode," in *Proceedings of ENVISAT and ERS Symposium*, (Salzburg, Austria), 2004.

12. R. Crapolicchio and P. Lecomte, "On the stability of Amazon Rainforest backscattering during the ERS-2 scatterometer mission lifetime," tech. rep., Serco/ESA, 2004.

13. S. M. Kay, *Modern Spectral Estimation: Theory and Application*, NJ: Prentice-Hall, Englewood Cliffs, 1987.

14. D. Long and M. Drinkwater, "Alternative large-scale distributed targets for SAR elevation beam pattern characterization," in *IEEE Transactions on Geoscience and Remote Sensing*, **Vol. 38, No. 4**, 2000.